

THE DISTRIBUTION OF GALAXIES WITHIN THE “GREAT WALL”

MASSIMO RAMELLA,^{1,2} MARGARET J. GELLER,² AND JOHN P. HUCHRA²*Received 1991 June 3; accepted 1991 July 22*

ABSTRACT

We examine the galaxy distribution within the “Great Wall,” the most striking feature in the first three “slices” of the CfA redshift survey extension. We extract the Great Wall from the sample and analyze it by counting galaxies in cells. We compute the “local” two-point correlation function within the Great Wall and estimate the local correlation length, s_0^{GW} . We obtain $s_0^{\text{GW}} \approx 15 h^{-1}$ Mpc, ~ 3 times larger than the correlation length for the entire sample (de Lapparent et al.).

The redshift distribution of galaxies in the pencil-beam survey by Broadhurst et al. shows peaks separated by large “voids,” at least to a redshift $z \approx 0.3$. The peaks might represent the intersections of their $\sim 5 h^{-1}$ Mpc pencil beams with structures similar to the Great Wall (Broadhurst et al.). Under this hypothesis, sampling of the Great Wall shows that $l \approx 12 h^{-1}$ Mpc is the minimum projected beam size required to detect all the “walls” at redshifts between the peak of the selection function and the effective depth of the survey. (We use a Hubble constant $H_0 = 100 h \text{ km s}^{-1} \text{ Mpc}$.)

Subject headings: cosmology: observations — galaxies: clustering — galaxies: distances and redshifts

1. INTRODUCTION

Three recent redshift surveys demonstrate the common occurrence of large-scale coherent features—voids and walls—in the galaxy distribution (Geller & Huchra 1989 (CfA hereafter); Broadhurst et al. 1990 (BEKS hereafter); Saunders et al. 1991). The largest voids in the CfA survey have diameters of $\sim 50 h^{-1}$ Mpc. In contrast, the deep probes of BEKS suggest that structures like the “Great Wall” (GW hereafter; CfA) are common and that they are typically separated by voids with a scale of $\sim 128 h^{-1}$ Mpc to a depth $z \approx 0.3$.

Here we examine the relationship between shallow redshift surveys covering a large solid angle and deep probes which subtend a very small solid angle. We ask whether the apparently larger voids in the deep probes are consistent with expectations based on sampling of the shallow surveys. One approach to exploring the characteristics of different redshift surveys is to use the results of n -body simulations or geometric models as a guide (White et al. 1987; Kurki-Suonio et al. 1990; Ikeuchi & Turner 1991). White et al. (1987) investigate the appearance of pencil beam surveys in biased cold dark matter simulations and comment: “Some directions show few galaxies and rather little structure. In others, large redshift intervals containing very few galaxies can be found. This diversity of structure is a result of the small transverse dimension of the surveys and of the strong small scale clustering of ‘galaxies.’”

De Lapparent, Geller, & Huchra (1991) take a more direct approach and consider the implications of the CfA survey for the appearance of pencil-beam surveys. They measure the average surface density in the “walls” and examine the sensitivity of pencil beams as a function of redshift. The average surface density they measure is approximately a factor of 2 less than the surface density corresponding to the peaks in the BEKS survey.

Here we argue that this difference is a result of clustering within the walls; the probes only detect walls when they

include dense regions occupied by groups and/or clusters. We take the suggestion of BEKS at face value and use the GW extracted from the CfA survey as a prototypical “wall.” We calculate the probability of “detection” as a function of beam size. Because galaxies are clustered within the wall, beams like those used by BEKS with an effective scale of $\approx 5 h^{-1}$ Mpc “detect” the wall only 40% of the time. Thus a typical void in a pencil-beam survey should appear larger than in the CfA survey. We show that a beam with an effective scale of $\approx 12 h^{-1}$ Mpc, comparable with the *local* correlation length within the wall, nearly always “detects” the structure.

In § 2 we describe the data and the procedure we use to “extract” the GW from the survey. In § 3 we sample the GW to obtain local values of thickness and galaxy density and we compare the results with a set of random simulations. In § 4 we direct random pencil beams through the GW and derive the probability of “detecting” a wall in the BEKS survey. We examine the expected dependence of the results of pencil-beam surveys on beam size. In § 5 we compute the “local” correlation function for galaxies within the GW and compare it with the “global” correlation function determined for the entire sample (de Lapparent, Geller, & Huchra 1988). We discuss the results in § 6.

2. DATA AND SELECTION OF THE GREAT WALL

2.1. *The Data*

The GW (Geller & Huchra 1989) is a large, bidimensional, connected structure in redshift space (de Lapparent et al. 1991). Its average overdensity is a factor ≈ 2.5 above the mean for the sample.

We analyze the portion of the GW contained in three adjacent slices of the Center for Astrophysics redshift survey extension (Geller & Huchra 1989). The three adjacent slices contain 2536 galaxies with $m_{B(0)} \leq 15.5$ and $cz \leq 15,000 \text{ km s}^{-1}$ and cover the right ascension range $8^{\text{h}} \leq \alpha \leq 17^{\text{h}}$ and the declination range $26.5^\circ \leq \delta < 44.5^\circ$. The solid angle is 0.60 steradians. The GW is still easily recognizable in the declination range $8.5^\circ \leq \delta < 14.5^\circ$. Because the GW (see Fig. 1) is at a mean redshift of $\sim 8000 \text{ km s}^{-1}$, corrections for departures from the

¹ Osservatorio Astronomico di Trieste, Via G.B. Tiepolo, 11, I-34131 Trieste, Italy.

² Harvard-Smithsonian Center for Astrophysics, 60 Garden Street, Cambridge, MA 02138.

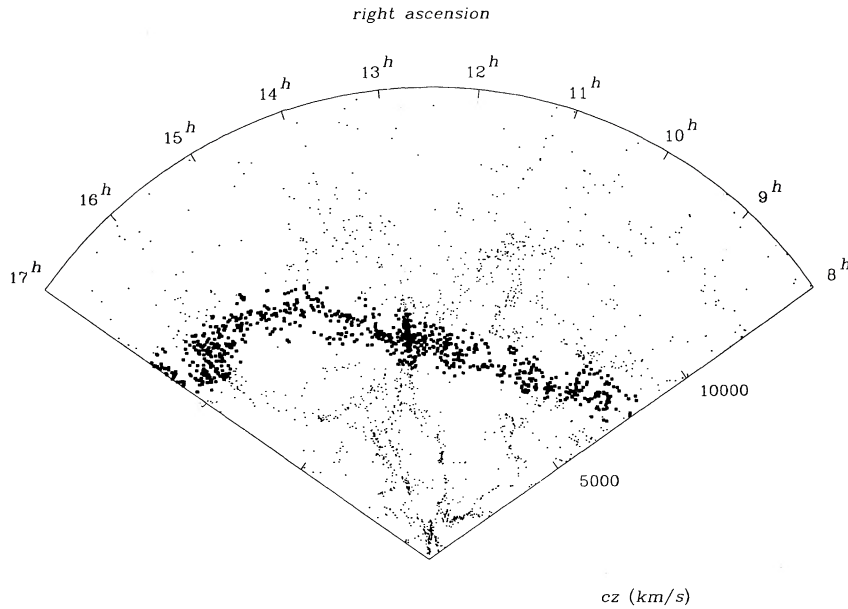


FIG. 1.—Cone diagrams for the declination range $26.5 \leq \delta \leq 44.5$. The plots contain 2536 galaxies with $m_{B(0)} \leq 15.5$ and $cz \leq 15,000 \text{ km s}^{-1}$. The squares mark 906 galaxies within the Great Wall.

Hubble flow in the neighborhood of our Galaxy have no effect on the analysis. We make no correction.

We use the luminosity function derived by de Lapparent, Geller, & Huchra (1989) for the first two slices of the CfA survey ($26.5 \leq \delta < 38.5$). The parameters for the Schechter (1976) form are

$$\begin{aligned} \phi^* &= 0.020 \text{ galaxies mag}^{-1} \text{ Mpc}^{-3} ; \\ M_{B(0)}^* &= -19.2 ; \quad \alpha = -1.1 . \end{aligned} \quad (1)$$

Groups and their membership are from Ramella, Geller, & Huchra (1989; RGH89 hereafter). To extend the analysis to the third slice we have applied the procedure described in RGH89 with the same group selection parameters.

2.2. Selection of the Great Wall

The cone diagram in Figure 1 shows the 906 galaxies in the GW (*larger symbols*) along with the rest of the galaxies in the survey (*smaller symbols*). Among the 906 galaxies in the GW, there are 416 members in 77 groups.

We selected the GW by visually inspecting cone diagrams. Over most of its extent ($\geq 80\%$), the GW is a high-contrast feature which does not intersect other structures. In these “clean” regions, the selection of the GW in redshift space is straightforward (e.g., de Lapparent et al. 1991). On the other hand, assignment of galaxies to the GW is rather arbitrary in the regions where there are intersections with other structures. Here we extrapolate the boundary across the intersection from the surrounding “clean” regions.

Our goal is the calculation of the surface number density of galaxies in the GW from the distribution of counts in cells. Our selection procedure cuts off some of the high-velocity members of the Coma Cluster, of A2197/99 and, possibly, of some other systems. We do not try to recover these members; for the scales of interest ($r \lesssim 15 h^{-1} \text{ Mpc}$), a cell containing Coma is in the tail of the distribution of counts in cells. The missing galaxies have a negligible effect on the analysis.

3. DISTRIBUTION OF GALAXIES WITHIN THE GREAT WALL

In this section we analyze the distribution of galaxies within the GW. We investigate the redshift distribution $n(cz)$ and the distribution of counts in cells on the plane of the sky. To obtain the local value of the number density of galaxies, $\rho(\alpha, \delta; \theta)$, we characterize the GW by counting galaxies in cells of angular size θ . Because the GW is thin and of nearly uniform thickness as measured by the local velocity dispersion, $\sigma_{cz}(\alpha, \delta; \theta)$, the function $\rho(\alpha, \delta; \theta)$ contains the information required to compare the GW with more distant structures like the ones detected in the BEKS probes.

De Lapparent et al. (1991) use the *average* surface density of the GW as a basis for their comparison of the GW with structures in the BEKS survey. Here we examine the effects of clustering within the GW on the comparison.

To examine the effect of clustering we construct 10 random samples. Each of these simulations consists of points drawn at random within the volume occupied by the GW. We use the selection function determined from the data (eq. [1]) but with a normalization appropriate to yield 906 points in the simulated “wall.”

3.1. The Redshift Distribution

Figure 2 shows the distribution of the velocities, $n(cz)$, for the galaxies within the GW (*solid line*). We also plot the corresponding histogram for a simulation (*dashed line*). The minimum velocity is 5890 km s^{-1} , very close to the peak of $n(cz)$; the maximum is $10,918 \text{ km s}^{-1}$. The mean cz is 7978 km s^{-1} , very close to the effective depth of the survey.

The GW is only $\sim 5 h^{-1} \text{ Mpc}$ thick and the mean position varies substantially across the survey. Figure 1 shows the slow variation of the mean velocity of the GW with right ascension. The thickness of the GW is a measure of the maximum variation of the mean velocity of the GW with declination. The systematic variation of the mean velocity with right ascension and the clustering of galaxies in the GW produce the double peak in $n(cz)$, a geometrical effect caused by the projection of a very wide angle ($\geq 100^\circ$) on the cz axis.

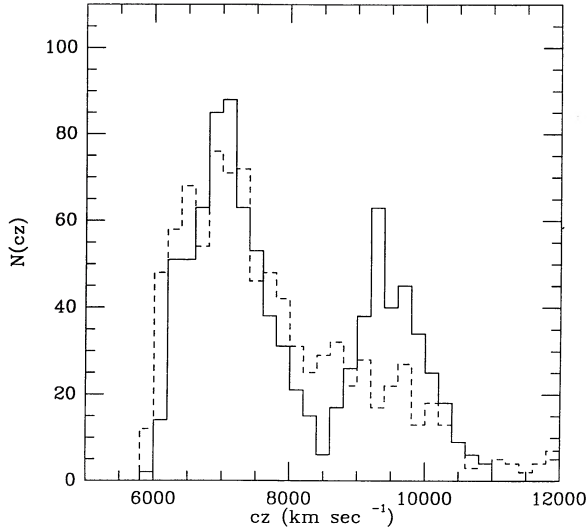


FIG. 2.—Redshift distribution of samples in the declination range $26:5 \le \delta \le 44:5$: Great Wall (solid line); random uniform simulation of the Great Wall (dashed line).

We measure the thickness of the GW by calculating the standard deviation of the velocities, $\sigma_{cz}(\alpha, \delta; \theta)$. We divide the area of the GW into adjacent cells of fixed angular extent, θ , and examine the distribution of $\sigma_{cz}(\theta)$ for cell sizes, θ , which correspond roughly to the correlation length for the galaxy distribution, $\sim 5\text{--}7 h^{-1}$ Mpc (de Lapparent et al. 1988). We examine $\sigma_{cz}(\theta)$ for $\theta = 3^\circ$ (4.5°), corresponding to projected scales of 4 (6) h^{-1} Mpc at the mean cz of the GW.

Figure 3 shows the distribution of $\sigma_{cz}(\theta = 3^\circ)$. We ignore cells which contain only one galaxy. The figure also shows the distribution for one of the random simulations. For both the GW and the simulation, Table 1 gives the mean, the rms fluctuation, and the median of the distributions $\sigma_{cz}(\theta = 3^\circ)$ and $\sigma_{cz}(\theta = 4.5^\circ)$. We also give the total number of cells, the number of cells which have at least two galaxies, and the number of cells with at least five galaxies.

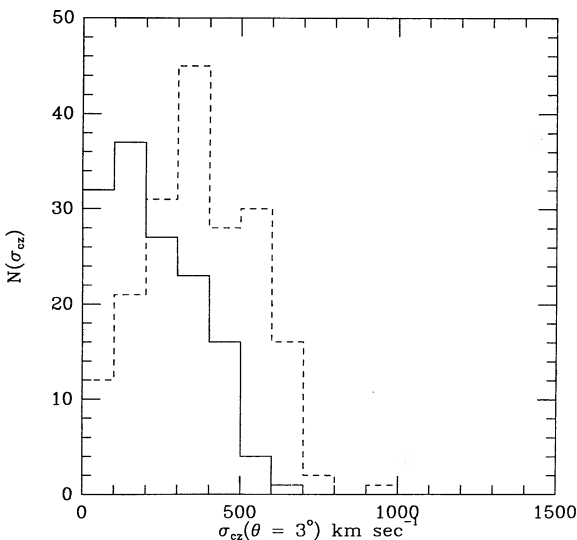


FIG. 3.—Distribution of the standard deviation in the velocities, $\sigma_{cz}(\alpha, \delta; \theta)$, in adjacent cells of angular extent $\theta = 3^\circ$ covering the Great Wall (solid line); the random uniform simulation of the Great Wall (dashed line).

TABLE 1
THE DISTRIBUTION OF $\sigma_{cz}(\alpha, \delta; \theta)$

CELL SIZE	NUMBER OF CELLS WITH N_{occ}			$\langle \sigma_{cz} \rangle$ (km s ⁻¹)	rms (km s ⁻¹)	MEDIAN (km s ⁻¹)
	≥ 0	≥ 2	≥ 5			
Great Wall						
$\theta = 3^\circ$	227	139	60	230	140	203
$\theta = 4.5^\circ$...	93	84	61	297	162	293
Simulation						
$\theta = 3^\circ$	227	194	61	374	172	360
$\theta = 4.5^\circ$...	93	93	84	449	133	453

The values of $\sigma_{cz}(\theta)$ for the simulation are generally larger than for the actual GW because the apparent thickness of the GW in a cone diagram is caused in part by variation of the mean cz in the declination direction (i.e., bending of the GW). Probably $\sigma_{cz}(\theta = 3^\circ)/\sigma_{cz}(\theta = 4.5^\circ) < 1$ because the gradient in mean velocity is less important for the smaller bin size.

The value of $\sigma_{cz}(\theta)$ is the same as the median velocity dispersion for groups of galaxies in the region, 216 km s^{-1} . If we remove members of these groups from the GW, both the median and mean σ_{cz} decrease slightly, but not significantly. For example, with $l = 4 h^{-1}$ Mpc, the median σ_{cz} drops from 203 km s^{-1} to 190 km s^{-1} and the mean from 230 km s^{-1} to 219 km s^{-1} . This coincidence between $\sigma_{cz}(\theta)$ for the GW and the median velocity dispersion for groups complicates group identification (RGH89).

The result we obtain for $\sigma_{cz}(\theta)$ agrees well with measures of the thickness based on simple geometric models (de Lapparent et al. 1991) for *all* of the structures in the survey (including but not limited to the GW). This analysis yields a FWHM of 500 km s^{-1} . The median velocity dispersion for $l = 4$ (6) h^{-1} Mpc, corresponds to a FWHM of 475 (688) km s^{-1} . The agreement between the two different approaches to measuring the thickness of the GW provides reassurance that any arbitrariness in our method of identifying the GW does not affect the quantitative results.

3.2. The Surface Distribution of Galaxies

The galaxy surface number density, $\rho(\alpha, \delta; \theta)$, is the basic parameter we use to compare the GW with other structures. The small and roughly constant thickness of the GW makes it reasonable to use the surface number density to characterize the distribution of galaxies in similar structures. The mean cz of the GW does vary across the survey, but we neglect this variation when we analyze the distribution with cells of constant angular size. This approach has no effect on the results for two reasons. First, we want to compare the GW with structures intersected by deep probes (beams) in surveys like that of BEKS; these beams have an angular size which is fixed a priori. Second, some of the decrease in galaxy counts with redshift caused by our magnitude-limited sample is balanced by the increasing volume of the intersection of the beam with the structure. De Lapparent et al. (1991) discuss this effect. Here we demonstrate the absence of any significant effect by sampling one of the simulations where the only reason for a dependence of counts on right ascension is the combination of the sampling of the luminosity function and the variation in the volume. Figure 4 shows the number of galaxies in cells with

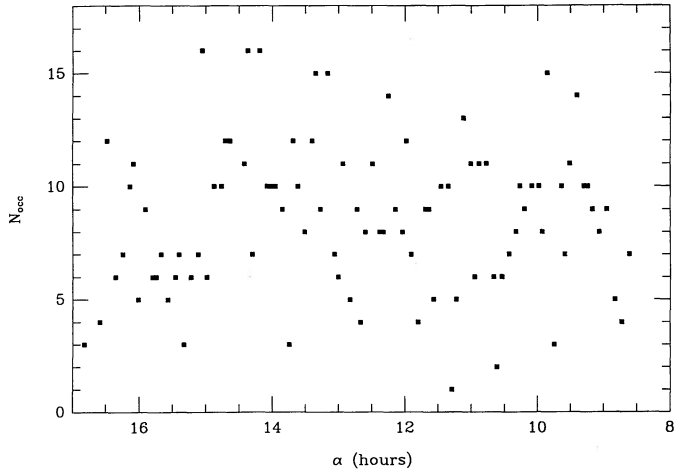


FIG. 4.—Occupation numbers, N_{occ} , of adjacent cells of angular extent $\theta = 4^\circ.5$ covering the Great Wall vs. the right ascension of the centers of the cells.

$\theta = 4^\circ.5$ as a function of right ascension: there is no significant variation.

Figure 5a shows the galaxies of the GW projected on the sky. Figures 5b and 5c show the occupation of $\theta = 4^\circ.5$ cells over the entire area of one of the simulations and of the GW, respectively. The cells cover an area of 1870 square degrees where there are 809 galaxies or 0.43 galaxies per square degree. In a uniform distribution we would expect an average of nine galaxies per cell. The light cells in the figures contain five or more galaxies. For the uniform simulations, these light cells cover, on average, $\sim 90\%$ of the area and contain 96% of the galaxies.

For the GW, the distribution is markedly different because of clustering: the light cells cover 65% of the total area but still contain 90% of the galaxies.

The distribution of occupation numbers for cells with $\theta = 4^\circ.5$ or $l = 6 \text{ h}^{-1} \text{ Mpc}$ is skewed toward lower occupation numbers than the simulations and has a substantial tail to higher occupation numbers. This tail is absent in the uniform

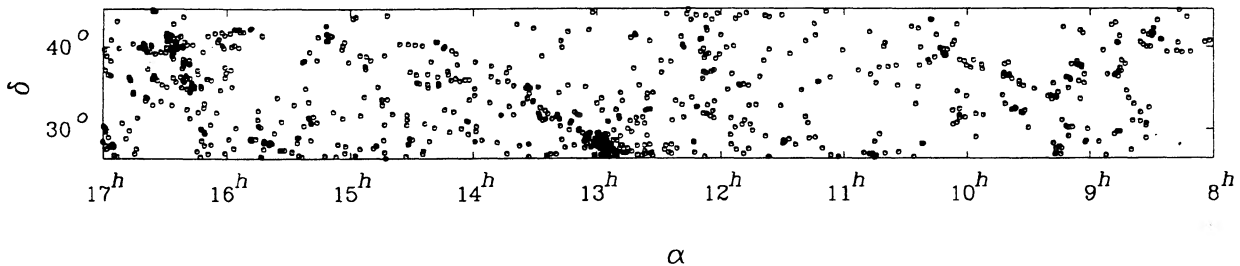


FIG. 5a

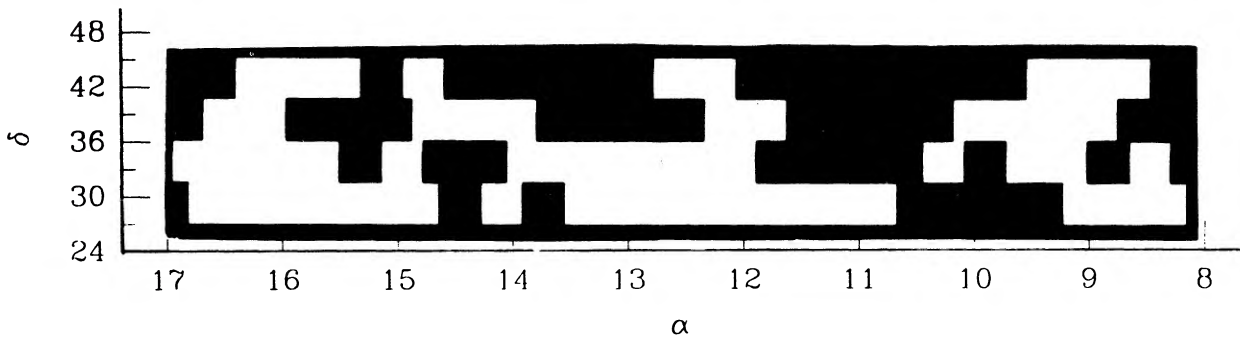


FIG. 5b

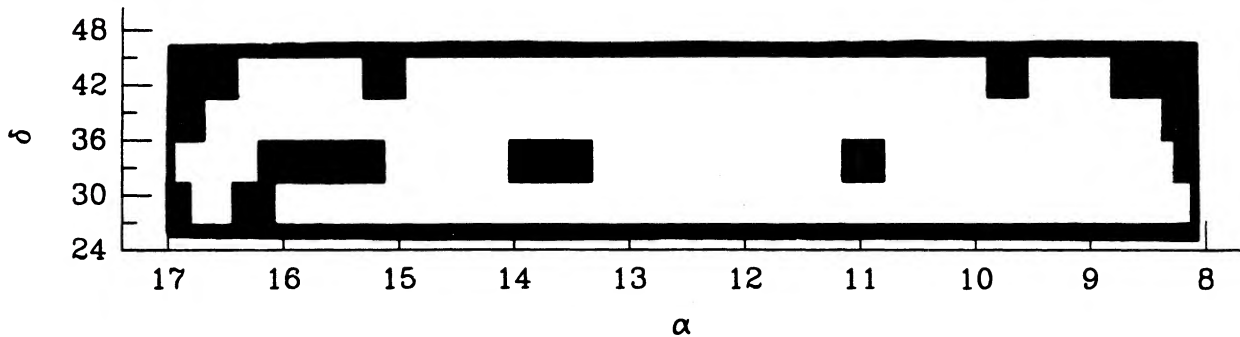


FIG. 5c

FIG. 5.—(a, b, c) Surface distribution of galaxies in the Great Wall (Fig. 5a). Figs. 5b and 5c, respectively, show the area of the Great Wall and of the simulation covered by adjacent cells of angular extent $\theta = 4^\circ.5$. The white cells are occupied by at least five galaxies, the black cells by less than five galaxies.

distribution. The median and the mean of the distribution for the simulations are both nine galaxies per cell. For the GW, however, the mean ($N_{\text{occ}} = 9$) is 55% larger than the median ($N_{\text{occ}} = 5$). The standard deviation of the distribution for the GW, $\sigma_N = 11$, is more than 3 times that for the simulations, $\sigma_N = 3.5$.

Groups (RGH89) have a high-density threshold and a scale of $\approx 1 h^{-1}$ Mpc. They populate the tail of the distribution at large N_{occ} and are responsible for the difference between the mean and the median N_{occ} .

Figure 6a summarizes the areal coverage of the GW (one of the simulations) as a function of cell size for cells occupied by N_{occ} or more galaxies. Figure 6b shows the percentage of galaxies contained in these cells. For the simulation, the dotted curves show a steep increase both of the areal coverage and of the fraction of galaxies contained in occupied cells for the two values of N_{occ} . The corresponding solid lines for the GW have considerably shallower slopes. For the simulation the areal coverage for cells with $N_{\text{occ}} > 0$ is almost 100% for $\theta \approx 3^\circ$ or $l \approx 2 h^{-1}$ Mpc, the mean interparticle spacing for both the simulation and the GW. For the GW nearly complete coverage occurs only when the cell size is about twice the mean interparticle spacing.

Thus, in a pencil-beam survey, the projected size of the probes must be larger than the mean intergalaxy spacing in order to detect at least one galaxy in the structure in each probe. Conversely, a densely occupied probe with a projected scale small compared with the average intergalaxy separation provides a substantial overestimate of the mean density of the intercepted structure.

4. THE GREAT WALL AND PENCIL-BEAM SURVEYS

Here we modify the counts-in-cells analysis to estimate the sensitivity of pencil-beam surveys to structures like the GW. We count galaxies in 1000 randomly placed cells of fixed angular extent. We do not count the beams with area outside the GW survey boundaries. Thus, as the size of the cells

increases, the number of cells we use to obtain the distribution of counts decreases. The smallest number of probes, for the largest cells, is 560. Here, because we do not “cover” the GW with adjacent cells, we can select any cell size. We vary l from $1 h^{-1}$ Mpc to $10 h^{-1}$ Mpc at the mean distance of the GW. This procedure effectively yields a smoothed version of the results in the previous section by increasing the number of samples at a given scale. We can then calculate the statistics of the distribution of cell occupation numbers, N_{occ} .

Figures 7a and 7b show results for the GW and one of the simulations, respectively. We plot the median count and several other percentiles of the count distribution as a function of cell size. At any cell size, the spread in N_{occ} is much larger for the GW than for the uniform control sample.

Because of the skewness of the distribution of N_{occ} for the GW, the median N_{occ} is less than the mean. For the simulation the median and mean N_{occ} are equal; the median N_{occ} for any cell size larger than the mean intergalaxy separation yields the correct mean galaxy surface density. For example, for $l = 3 h^{-1}$ Mpc the median is two galaxies or $0.22 \text{ galaxies } h^2 \text{ Mpc}^{-2}$; for $l = 10 h^{-1}$ Mpc the median is 23 galaxies or $0.23 \text{ galaxies } h^2 \text{ Mpc}^{-2}$. The global mean value is $0.23 \text{ galaxies } h^2 \text{ Mpc}^{-2}$ (in agreement with the typical surface density of structures in the redshift survey derived by de Lapparent et al. 1991). For the same cell sizes, the median occupation numbers for the GW are one and 15 galaxies, respectively, yielding surface densities of $0.11 \text{ galaxies } h^2 \text{ Mpc}^{-2}$ and $0.15 \text{ galaxies } h^2 \text{ Mpc}^{-2}$, significantly lower than the global mean.

The frequency distributions of N_{occ} yields estimates of the probability of obtaining $\geq N_{\text{galaxies}}$ in a single random pencil-beam intercepting a structure like the GW. Most of the peaks identified as “walls” by BEKS contain at least five galaxies and in some cases more than 10. Figure 8 shows the probability of finding at least five and at least 10 galaxies as a function of the size of the beam for the GW and for the simulation.

With increasing beam size, the probability of finding at least five or 10 galaxies approaches 100%. The probability increases

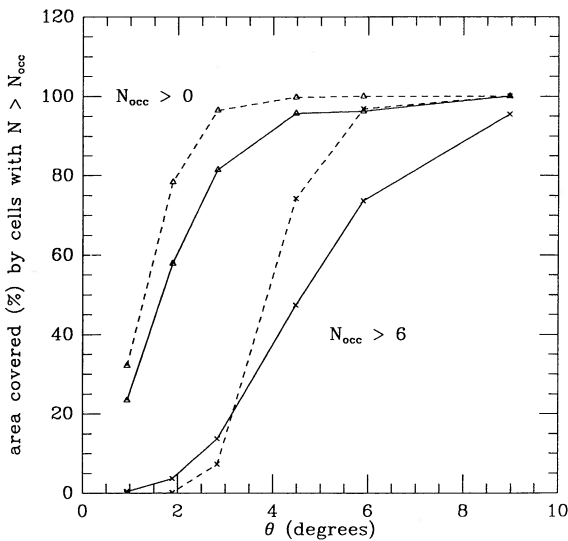


FIG. 6a

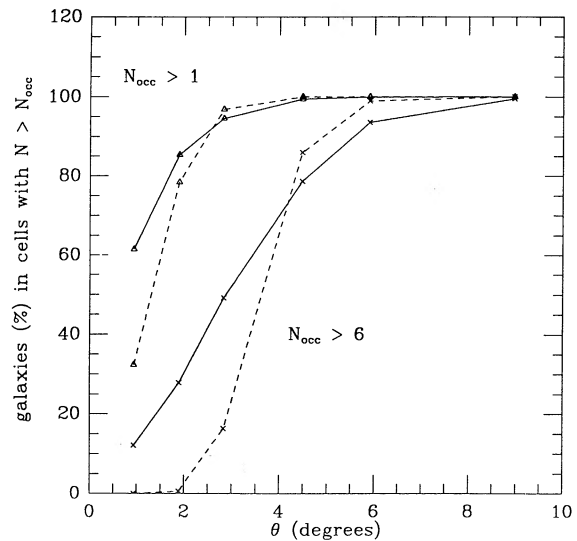


FIG. 6b

FIG. 6.—(a) Percentage of the area of the samples covered by cells of angular extent θ occupied by at least one (triangles) and at least seven (crosses) galaxies. Great Wall (solid line) and random uniform simulation of the Great Wall (dashed line).

FIG. 6.—(b) Percentage of the total number of galaxies of the samples contained in cells of angular extent θ occupied by at least two (triangles) and at least seven (crosses) galaxies. Great Wall (solid line) and random uniform simulation of the Great Wall (dashed line).

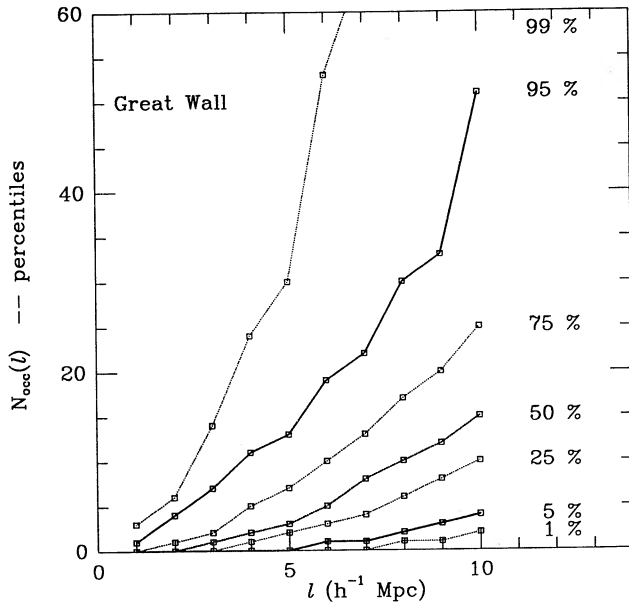


FIG. 7a

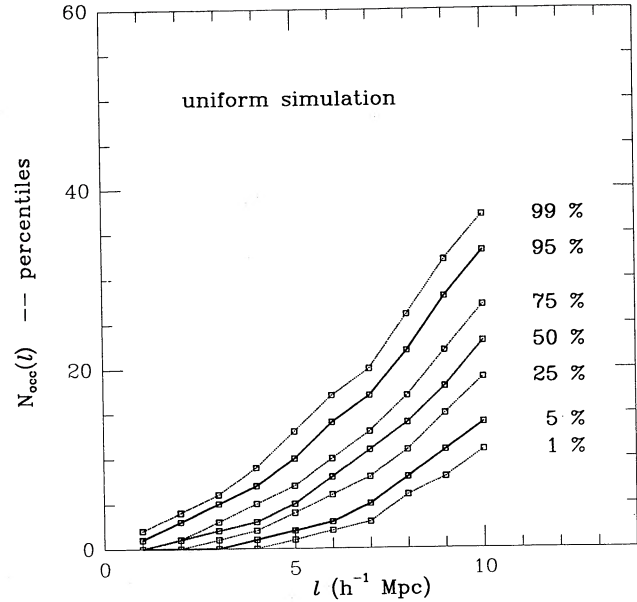


FIG. 7b

FIG. 7.—Percentiles of the distributions of the occupation numbers of cells of linear size l (at the mean distance of the Great Wall). (a) Great Wall; (b) random uniform simulation of the Great Wall.

faster for the simulation than for the GW. In the simulation, a beam with $l \gtrsim 7 h^{-1}$ Mpc always contains at least five galaxies. When probing the GW, the size of the beam must be greater than $\sim 12 h^{-1}$ Mpc to “ensure” the inclusion of at least five galaxies. Most of these beams will include 10 galaxies.

If the structures detected in the pencil-beam survey by BEKS are similar to the GW, than the probability of detection (Fig. 8) can be read as the fraction of “walls” detected in the redshift range $0.2 \lesssim z \lesssim 0.35$. Within these redshift limits the beam of BEKS has an effective linear scale, l , in the range $5 h^{-1}$ Mpc $\lesssim l \lesssim 7 h^{-1}$ Mpc. With such a beam 25%–60% of the

structures might be missed and the sizes of the “voids” correspondingly overestimated.

5. THE “LOCAL” GALAXY-GALAXY CORRELATION LENGTH

The two-point galaxy-galaxy correlation function, ξ_{gg} , also yields a qualitative limit on the minimum size that a pencil-beam survey must have in order to detect structures like the GW. For the CfA survey, de Lapparent et al. (1988) fitted the unweighted estimate of ξ_{gg} to a power law, $\xi_{gg} = (s/s_0)^\gamma$, in the range $3 h^{-1}$ Mpc $< s < 10 h^{-1}$ Mpc. They obtain $s_0 \approx 5 h^{-1}$ Mpc, $\gamma \approx -1.7$ in close agreement with the values used by BEKS (Shanks et al. 1983). The symbol s is the separation of pairs in redshift space.

The sampling experiments in the previous section show that a beam with $l \gtrsim 12 h^{-1}$ Mpc surely detects the GW. This value of l is larger than s_0 by a factor 2.5; a beam with the $l \approx 5 h^{-1}$ Mpc “misses” the wall about 60% of the time, contrary to naive expectations based on the galaxy correlation function. The reason for this result is that the correlation length *within the GW*, or “local” correlation length s_0^{GW} , is the relevant scale in the problem.

To compute the correlation function for the GW, ξ_{gg}^{GW} , we construct a control sample with points randomly distributed within the same volume as the GW. We distribute the points according to the proper selection function scaled to yield the number of points observed in the GW. As usual (e.g., Davis & Peebles 1983) we use

$$\xi_{gg}^{GW}(s) = \frac{N_{DD}(s)}{N_{DR}(s)} - 1$$

as the estimator of $\xi(s)$. $N_{DD}(s)$ is the number of pairs at a separation $(s, s + ds)$ in the GW. N_{DR} is the number of pairs at separation $(s, s + ds)$ with one point in the data GW and the other in the random control sample.

Figure 9 shows $\log(\xi_{gg}^{GW})$ as a function of $\log(s)$. We also plot $\log(\xi_{gg}^{GW})$ (de Lapparent et al. 1988). The amplitude of $\log(\xi_{gg}^{GW})$

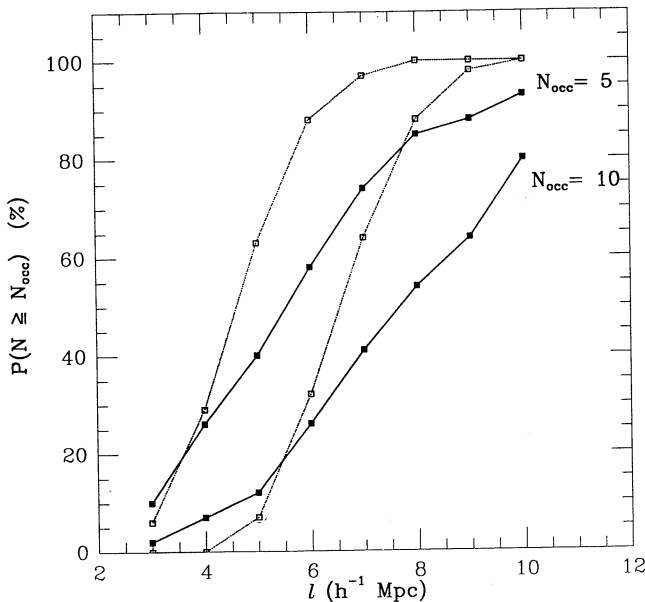


FIG. 8.—Probability of counting at least five (at least 10) galaxies in a beam of linear size l intercepting Great Wall (solid line) and the random uniform simulation of the Great Wall (dotted line).

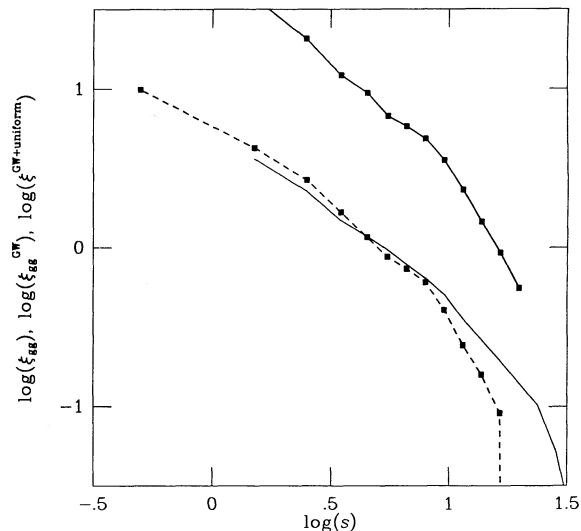


FIG. 9.—Two-point correlation functions for the Great Wall (*thick solid line with squares*); for the whole sample as measured by de Lapparent et al. (1988) (*thick dashed line with symbols*); for the sample containing the Great Wall and a uniform distribution of random points (*solid line*).

is almost one order of magnitude larger than the amplitude of ξ_{gg} ; in other words $s_0^{GW}/s_0 \approx 3$. The slopes are remarkably similar.

The larger amplitude of ξ_{gg}^{GW} compared with ξ_{gg} means the signal produced by the GW is diluted by the galaxy distribution in the rest of the survey volume. About $\frac{1}{3}$ of the galaxies in the whole sample are in the GW; the remaining $\frac{2}{3}$ may as well be randomly distributed (Fig. 10). We verify this argument by adding uncorrelated galaxies to those within the GW; we construct a composite sample with the same number of galaxies as in the CfA survey “slices,” and within the same boundaries. The amplitude of the correlation function for this “sample” is the same as for the data (Fig. 9)!

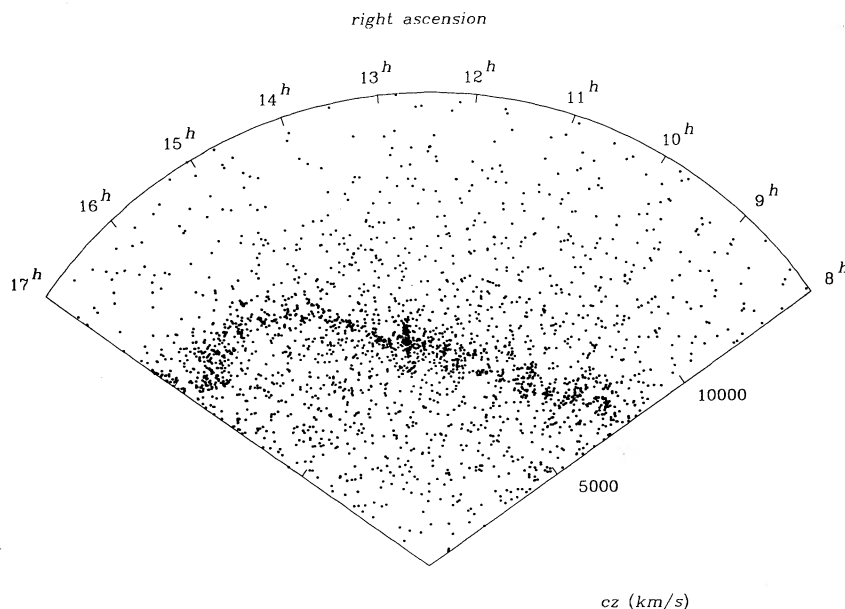


FIG. 10.—Cone diagram for the composite sample containing the Great Wall and a uniform distribution of random points. The number of points in the composite sample matches that of the observed “slices” in the declination range $26^\circ.5 \leq \delta \leq 44^\circ.5$. Note the contrast with Fig. 1; the correlation functions for these two distributions are the same (Fig. 9).

The *local* correlation length $s_0^{GW} \approx 15 h^{-1}$ Mpc is comparable with the beam size required to detect the GW in the sampling experiments of §§ 3 and 4. The variance of counts in a pencil beam is proportional to the correlation length (Szalay et al. 1991); the particular correlation length which affects the detection of a GW is s_0^{GW} , not s_0 . Calculation of the variance based on s_0 (see, e.g., BEKS) underestimates the variance of counts in the intercepted GW and correspondingly overestimates the significance of “voids” between peaks.

6. CONCLUSION

The pencil-beam surveys of BEKS suggest that structures like the GW might be common in the universe, at least to a redshift $z \approx 0.3$. Interpretation of the results of these surveys depends upon an estimate of the probability of “detecting” a “wall.”

We explore the problem by extracting the GW from the CfA survey and using it as a template for more distant walls. Our results are insensitive to the details of the extraction of the GW; analysis of the entire sample in the velocity range $6000 \text{ km s}^{-1} \leq cz \leq 12,000 \text{ km s}^{-1}$ yields the same results. By direct experiment, we evaluate the probability of detecting a wall as a function of the opening angle of the pencil beams.

These experiments yield measures of the statistical properties of the GW in agreement with previous analyses using other techniques (de Lapparent et al. 1991). The average surface density of the GW is $0.23 \text{ galaxies } h^2 \text{ Mpc}^{-2}$ and the FWHM is $\approx 500 \text{ km s}^{-1}$.

Our approach also confirms the visual impression that the GW is a bidimensional connected structure. Smoothing on a scale of $\lesssim 10 h^{-1}$ Mpc, i.e., $1/10$ of the largest linear dimension of the GW, produces a “solid” wall; i.e., all cells are occupied at the 3σ level. On small scales, $l \lesssim 2 h^{-1}$ Mpc, systems of galaxies dominate the “local” texture of the GW. Almost half of the galaxies within the GW are members of groups or clusters.

Using the GW as a guide, we obtain a lower limit on the projected linear scale of beams which always detect a "wall." For each beam scale, we choose 1000 random samples through the GW and count the galaxies "intercepted" by the beam. The "safe" size of the beam is about $12 h^{-1}$ Mpc, i.e., almost a factor 3 larger than the correlation length for the entire sample ($s_0 \simeq 5 h^{-1}$ Mpc). This scale is comparable with the local correlation length $s_0^{\text{GW}} \simeq 15 h^{-1}$ Mpc $\simeq 3 s_0$.

At redshifts between the peak of the selection function and the effective depth of the survey, beams with a scale of $\simeq 5 h^{-1}$ Mpc will detect the "walls" only 40% of the time. The probability of detecting "walls" is a factor of $1/\cos i$ larger for beams intersecting "walls" with a random inclination angle i (Szalay et al. 1991). However, because the scale of the beams and the thickness of the walls are small ($< 1/10$) compared to the size of "voids," most of the beams intersect "walls" which are effectively perpendicular to the line of sight.

Because "walls" are missed, the scale of intervening "voids" is overestimated. In fact, the typical spacing between the "walls," λ , can be estimated from the mean surface density μ of

the GW and the global mean density of the survey n : $\lambda = 3\mu/n$ (Szalay et al. 1991). With the galaxy densities derived for the GW and the CfA survey, $\mu \simeq 0.25$ galaxies $h^2 \text{ Mpc}^{-2}$ (this paper) and $n \simeq 0.02$ galaxies $h^3 \text{ Mpc}^{-3}$ (de Lapparent et al. 1989), the typical spacing is $\lambda \simeq 40 h^{-1}$ Mpc, in good agreement with the CfA "slices." This scale is also consistent with the hypothesis that the scale $\lambda \simeq 100 h^{-1}$ Mpc found by BEKS is larger because of missing "walls."

Finally, because the distribution of occupation numbers of the cells has a large tail toward high occupation numbers (Fig. 7a), the detection of a wall with a narrow beam will frequently lead to an overestimate of the galaxy density in the wall itself. These effects explain why the scale of voids is larger and the effective surface density of the peaks is greater in deep probes than in shallow large solid angle surveys.

We thank Alex Szalay and Gianni Zamorani for discussions. This work is supported in part by NASA grant NAGW-201, the Smithsonian Scholarly Studies Program, and the Italian CNR.

REFERENCES

- Broadhurst, T. J., Ellis, R. S., Koo, D. C., & Szalay, A. S. 1990, MNRAS, 343, 726 (BEKS)
 Davis, M., & Peebles, P. J. E. 1983, ApJ, 267, 465
 de Lapparent, V., Geller, M. J., & Huchra, J. P. 1986, ApJ, 302, L1
 ———. 1988, ApJ, 332, 44
 ———. 1989, ApJ, 343, 1
 ———. 1991, ApJ, 369, 273
 Geller, M. J., & Huchra, J. P. 1989, Science, 246, 879
 Ikeuchi, S., & Turner, E. L. 1991, MNRAS, in press
 Kurki-Suonio, H., Mathews, G. J., & Fuller, G. M. 1990, ApJ, 356, L5
 Ramella, M., Geller, M. J., & Huchra, J. P. 1989, ApJ, 344, 57 (RGH89)
 Saunders, W., et al. 1991, Nature, 349, 32
 Schechter, P. 1976, ApJ, 203, 297
 Shanks, T., Bean, A. J., Efstathiou, G., Ellis, R. S., Fong, R., & Peterson, B. A. 1983, ApJ, 274, 529
 Szalay, A. S., Ellis, R. S., Koo, D. C., & Broadhurst, T. J. 1991, in After the First Three Minutes, ed. S. Holt et al. (New York: AIP)
 White, S. D. M., Frenk, C. S., Davis, M., & Efstathiou, G. 1987, ApJ, 313, 505